Available online at www.sciencedirect.com
SCIENCE DIRECT®
Applied Catalysis A: General 278 (2005) 239–249
APPLIED CATALYSIS A: GENERAL
www.elsevier.com/locate/apcata

XPS and EXAFS study of supported PtSn catalysts obtained by surface organometallic chemistry on metals Application to the isobutane dehydrogenation

Guillermo J. Siri[a,b], José M. Ramallo-López[c], Mónica L. Casella[a], José L.G. Fierro[d], Félix G. Requejo[c], Osmar A. Ferretti[a,b,*]

[a]*Centro de Investigación y Desarrollo en Ciencias Aplicadas "Dr. Jorge Ronco" (CINDECA), Facultad de Ciencias Exactas, Universidad Nacional de La Plata, 47 No. 257 (1900) La Plata, Argentina*
[b]*Departamento de Ingeniería Química, Facultad de Ingeniería, Universidad Nacional de La Plata, 47 No. 257 (1900) La Plata, Argentina*
[c]*Instituto de Física de La Plata (IFLP) (CONICET) and Departamento de Física, Facultad de Ciencias Exactas, Universidad Nacional de La Plata, 49 y 115 (1900) La Plata, Argentina*
[d]*Instituto de Catálisis y Petroleoquímica, CSIC, Cantoblanco, E-28049 Madrid, España*

Received 19 May 2004; received in revised form 30 September 2004; accepted 2 October 2004
Available online 18 November 2004

Abstract

In this work, well defined alumina and silica supported Pt and PtSn catalysts were prepared by surface organometallic reactions and were characterized by TEM, XPS and EXAFS. These catalysts were tested in the catalytic dehydrogenation of isobutane. XPS results show that tin is found under the form of Sn(0) and Sn(II,IV), being the percentage of Sn(0) lower for alumina supported than for silica supported catalysts. Tin modified platinum catalysts, always show a decrease of approximately 1 eV in the BE of Pt, what would be indicative of an electron charge transfer from tin to platinum. When the concentration of Sn(0) is high enough, in our case Sn(0)/Pt $\sim$ 0.3, EXAFS experiments demonstrated the existence of a PtSn alloy diluting metallic Pt atoms, for both PtSn/γ-Al_2O_3 and PtSn/SiO_2. This PtSn alloy seems to be not active in the dehydrogenation reaction; however, it is very important for selectivity and stability, inhibiting cracking and coke formation reactions. The ensemble of our catalytic, XPS and EXAFS results, show that bimetallic PtSn/γ-Al_2O_3 catalysts, prepared via SOMC/M techniques, can be submitted to several sequential reaction–regeneration cycles, recovering the same level of initial activity each time and that the nature of the catalytic surface remains practically without modifications.

Keywords: PtSn catalysts; Organometallic chemistry; Isobutane hydrogenation; Catalyst regeneration

1. Introduction

Light olefins are widely employed in industry, as they are involved in processes such as production of polymers, ethers, nitriles, new gasolines, etc. Most of these olefins are obtained as by-products of both thermal and catalytic cracking processes, and so, the volume of gasoline required by the market determines the availability of olefins. The deficit is covered at the present time by means of the catalytic dehydrogenation of light paraffins.

The dehydrogenation of light paraffins to olefins is an endothermic reaction; that it is why it requires the application of relatively severe operation conditions (temperature above 500 °C in the case of isobutane). Under these conditions, mono and bimetallic catalytic systems based on Pt/γ-Al_2O_3 lead to undesirable reactions, such as the formation of light cracking and isomerization products and coke deposits, all of them responsible for the loss of selectivity and activity of the catalysts. This kind of

* Corresponding author. Tel.: +54 221 421 0711; fax: +54 221 425 4277.
E-mail address: ferretti@quimica.unlp.edu.ar (O.A. Ferretti).

0926-860X/$ – see front matter © 2004 Elsevier B.V. All rights reserved.
doi:10.1016/j.apcata.2004.10.004

deactivation is reversible and the regeneration of the solid can be carried out by burning the coke formed under controlled conditions. In each regeneration cycle, the temperature reaches a value high enough so as to cause sintering of the metallic phase and, in the case of multimetallic catalysts, the segregation of the metals can also take place, causing an irreversible deactivation of the catalyst [1,2].

Pt/γ-Al_2O_3 catalysts are active in the paraffins dehydrogenation process, but they deactivate very quickly and have a poor selectivity towards olefins, mainly caused by the existence of cracking and isomerization reactions. Cracking reactions are promoted by metallic active sites, while isomerization reactions not only are activated on these sites, but also on the acid sites of the support. It has been shown that the addition of alkaline and alkaline-earth ions to γ-Al_2O_3 selectively poisons the isomerization active sites, without affecting the dehydrogenation capacity of the catalytic systems [3–5].

The addition of tin to Pt/γ-Al_2O_3 catalysts notably increases the stability and selectivity for dehydrogenation of paraffins to olefins, inhibiting cracking and isomerization reactions and coke formation process [2,3,6–9]. Tin is said to act to modify platinum by an ''ensemble effect'', decreasing the number of contiguous platinum atoms, dividing the platinum surface into smaller ensembles; in this way hydrogenolysis and deactivation by coke deposition are drastically reduced. A second effect is of an electronic nature: the presence of tin changes the electronic environment of platinum atoms [9–12].

The accurate nature of PtSn systems is very complicated and still a matter of debate, but any proper explanation of the role of tin in PtSn/γ-Al_2O_3 catalysts is necessarily related to the oxidation state of tin. The state of tin depends on catalyst preparation, metal loadings, Sn/Pt ratio, support and activation treatments [3,11–17], therefore contradictory results are not surprising. To completely characterize the electronic state of the metals, their geometrical array and the nature of the interaction between them, it becomes necessary to employ sophisticated analytical techniques, such as XPS, Mössbauer spectroscopy and EXAFS. EXAFS spectroscopy gives information about the surroundings of the absorber atom. In the particular case of Pt, the study of the L_3 absorption edge measuring the transmission of X-rays, provides information about the kind, number and distance of neighbors around the Pt atoms.

Results published by Dautzemberg et al. [18] in the *n*-hexane conversion reaction, indicate that the bimetallic catalyst contains isolated Pt particles, together with Pt- and Sn-rich alloys; PtSn alloys are supposed to be responsible for the inhibition of the reactions taking place on active sites composed of a relatively high number of platinum atoms, whereas dehydrogenation reactions (which can proceed over small ensembles of Pt atoms) are not affected. XPS results obtained on PtSn/γ-Al_2O_3 catalysts show that an important proportion of tin is present under a ionic state, contrary to what happens with silica-supported catalysts, where important quantities of Sn(0) can be formed [19]. Other study, carried out by Lieske and Völter, concluded that in a series of PtSn/γ-Al_2O_3 catalysts, the major part of tin was present as Sn(II,IV), being this state stabilized by alumina [20]. Merlen et al. found that bimetallic PtSn phases supported on γ-Al_2O_3 are more easily obtained for larger particles than for small ones [7]. These authors suggested that the metallic particles may be too small to stabilize tin in the metallic state and tin probably migrates onto the support remaining in ionic state in the vicinity of the particle. Based on Mössbauer spectroscopy and XRD data for supported PtSn catalysts, Li et al. found that Sn(0) is alloyed with Pt [21]. Cortright et al., using Mössbauer spectroscopy for the characterization of PtSn/SiO_2 catalyst, observed a single dominant peak at a chemical shift of 1.83 mm/s which they assigned to the presence of Sn(0) alloyed with platinum [10]. PtSn/C catalysts were studied by EXAFS by Román-Martínez et al. [15]; the authors observed the presence of bimetallic PtSn phases, Pt particles, and Pt–O–Sn^{2+} species, suggesting that the catalytic activity of bimetallic catalysts is determined by the relative concentration of these surface species and their distribution in the support.

The influence of the preparation procedure is well depicted in a paper of Vértes et al., who studied by Mössbauer spectroscopy a series of PtSn/γ-Al_2O_3 catalysts prepared via Surface Organometallic Chemistry on Metals (SOMC/M) techniques reacting $Sn(C_2H_5)_4$ on Pt/γ-Al_2O_3 and by a conventional procedure, impregnating Pt/γ-Al_2O_3 with a $SnCl_2$ solution [13]. Their results showed that while as a consequence of the first-mentioned procedure tin was interacting with Pt in a superficial $PtSn_x$ alloy, the second procedure gave rise to a catalyst where the major part of tin was in an ionic state. The difference in the catalytic surface is correlated with a different catalytic behavior, as it was demonstrated in a previous work carried out by our research group in the isobutane dehydrogenation, where we presented some results indicating that PtSn/γ-Al_2O_3 prepared via SOMC/M gave a better yield to isobutene than bimetallic catalysts prepared using conventional impregnation procedures [8]. Besides, when the metals are introduced by coimpregnation of H_2PtCl_6 and $SnCl_2$, the resulting catalyst did not show good regenerability properties [1]. On the other hand, when bimetallic catalysts are prepared by SOMC/M techniques, the nature of the active phase formed can be accurately controlled leading to more selective catalysts that, in addition, can be regenerated, recovering the initial activity of the fresh catalysts [22]. This last characteristic of PtSn catalysts is a very important one, for even though Sn is an efficient promoter employed in industrial catalysts, deactivation due to coke is not completely eliminated and the catalysts still exhibit short lifetimes and it is necessary to submit them to continuous regeneration to maintain activity.

In this paper we use XPS and EXAFS to examine the evolution of the electronic state and the local structures of Pt and Sn in PtSn catalysts submitted to several

reaction–regeneration cycles in the isobutane dehydrogenation reaction. The aim of this work is to obtain accurate evidences concerning the nature and the stability of the active sites obtained when SOMC/M preparation techniques are employed.

2. Experimental

2.1. Catalyst preparation

A commercial γ-Al_2O_3 (Cyanamid Ketjen) crushed to a size of 60–100 mesh and a Degussa silica (Aerosil 200, 200 $m^2\ g^{-1}$) were used as supports. For the preparation of the platinum monometallic catalysts a solution of H_2PtCl_6 was added onto the γ-Al_2O_3 and a solution of $[Pt(NH_3)_4]^{2+}$ was added on functionalized silica. In both cases the solution had a concentration so as to obtain 1% (w/w) Pt exchanged on the support. Then, the solids were repeatedly washed, dried at 105 °C, calcined in air at 500 °C and reduced in flowing H_2 at the same temperature, leading to the monometallic Pt/γ-Al_2O_3 and Pt/SiO_2 catalysts. After the reduction step, the Pt/γ-Al_2O_3 catalyst was washed several times with NH_3 solution (0.1 M) at room temperature, in order to obtain a chlorine concentration under 0.1% in the resulting solid. The bimetallic systems have been prepared by reaction between the monometallic catalyst and different quantities of $SnBu_4$ dissolved in *n*-heptane, maintaining a H_2 flow of 30 $cm^3\ min^{-1}$ and a temperature of 90 °C during the reaction time, for the catalysts with Sn/Pt ratios up to 0.4. In the preparation of the catalysts with higher tin contents, *n*-decane was used as solvent and the reaction temperature was 150 °C. After 4 h of reaction, the systems were cooled to room temperature and were repeatedly washed with *n*-heptane under a H_2 atmosphere. This preparation procedure gives rise to an organometallic supported phase, which retains on the platinum surface part of the butyl groups of the $SnBu_4$. The elimination of the organic groups heating the solids in a H_2 atmosphere at 500 °C, generates the supported bimetallic catalysts PtSn. Platinum and tin contents were determined by atomic absorption spectrometry.

2.2. Characterization

2.2.1. Transmission electron microscopy (TEM)

The size distribution of metallic particles was determined by using a Jeol 2010 instrument. To estimate the mean particle size (d_{va}) the particles were considered spherical and the second moment of the distribution was employed.

2.2.2. Temperature programmed reduction (TPR)

The catalysts was performed by means of a conventional equipment using a programmable furnace and the response was measured using a thermal conductivity detector. The composition of the feed flow was $H_2/N_2 = 1/9$ and the heating rate was 10 °C min^{-1} from room temperature to 800 °C.

2.2.3. X-ray photoelectron spectroscopy (XPS)

The samples were re-reduced in situ in the pre-treatment chamber of the spectrometer. The spectra were obtained with a VG ESCALAB 200R spectrometer equipped with a hemispherical electron analyzer and a Mg Kα 120 W X-ray source. The reduction treatment was carried out in situ, by heating the fresh and postreaction samples under a hydrogen flow at 500 °C for 1 h. As internal standard, for alumina supported catalysts binding energy (BE) of the Al 2p peak at 74.5 eV and for silica supported catalysts the C 1s peak at 284.6 eV, were taken. The intensities were estimated by calculating the integral of each peak after subtraction of the S-shaped background and fitting the experimental peak to a Lorentzian/Gaussian mix of variable proportion.

2.2.4. X-ray absorption spectroscopy

The X-ray absorption spectra were measured at the XAS beam line at the National Synchrotron Light Laboratory (LNLS), Campinas, Brazil. The EXAFS spectra of the Pt L_3-edge (11.6 keV) were recorded at room temperature using a Si(1 1 1) crystal monochromator in the range 11 460–12 600 eV in transmission mode. Samples were sealed in H_2 atmosphere in special sample holders with kapton windows in order to avoid contact with air and were measured in that condition.

The EXAFS data were extracted from the measured absorption spectra by standard methods [23,24]. Raw data files were averaged and the preedge region was approximated by a polynomial curve. Normalization was completed dividing by the height of the absorption edge and the background was subtracted using cubic spline routines. The main contributions to the spectra were isolated on the Fourier transforms of the final EXAFS functions. The phase shifts and the amplitude functions for Pt–Pt and Pt–Sn pairs were calculated using the FEFF [25] program from the metallic Pt and PtSn alloy structure [26].

2.3. Activity measurements

The test reaction was the isobutane dehydrogenation. Activity test was performed by placing the sample in a conventional flow reactor at atmospheric pressure and 550 °C. The temperature of the reactor was raised to 550 °C with a heating rate of 10 °C min^{-1} under H_2 flow. This condition was mantained for 2 h, and then the reactor was fed with a mixture of H_2 and isobutane with a ratio H_2/isobutane = 3 and a total gas flow of 50 $cm^3\ min^{-1}$. The composition of the reaction products was analyzed using a Carlo Erba Fractovap series 2150 gas chromatograph on line with the reactor (tricresyl phosphate on Chromosorb W column). In all the tests, conversion was kept below 10% to assure kinetic control conditions (equilibrium conversion for these experimental conditions is around 55%).

Table 1
Composition and denomination of the studied catalysts

Catalyst	Support	Pt (wt.%)	y (mol $SnBu_4$ reacted in reaction (1))	Sn/Pt (at/at)
PtA	γ-Al_2O_3	1.0	0	0
PtS	SiO_2	1.0	0	0
PtSnA0.06[a]	γ-Al_2O_3	1.0	0.06	0.06
PtSnA0.12[a]	γ-Al_2O_3	1.0	0.12	0.12
PtSnA0.25[a]	γ-Al_2O_3	1.0	0.25	0.25
PtSnA0.4[a]	γ-Al_2O_3	1.0	0.40	0.40
PtSnA0.8[b]	γ-Al_2O_3	1.0	0.80	0.80
PtSnA1.6[b]	γ-Al_2O_3	1.0	1.60	1.60
PtSnS0.4[a]	SiO_2	1.0	0.40	0.40
PtSnS0.7[b]	SiO_2	1.0	0.70	0.70

[a] Prepared at 90 °C.
[b] Prepared at 150 °C.

Catalysts were submitted to a series of reaction–regeneration cycles. Coke deposit on fresh samples was carried out by means of a 4.5 h isobutane dehydrogenation reaction run, under the following conditions: atmospheric pressure, 550 °C and a feed flow of pure isobutane of 50 cm^3 min^{-1}. Then, the hydrocarbon feeding was replaced by an inert steam (Ar), simultaneously cooling the reactor up to 250 °C. Once this temperature has been reached, Ar was replaced by an air flow and the temperature was raised up to 550 °C, with a heating rate of 5 °C min^{-1}. After 1 h under this condition, the samples were cooled to room temperature, and kept that way overnight. In this way, samples are ready to be use in a new cycle.

3. Results

Table 1 shows the composition and the nomenclature of the catalysts investigated in the present study. The synthesis of bimetallic catalysts can be represented by the following global reaction:

$$\mathrm{Pt/support} + y\mathrm{SnBu_4} + \frac{1}{2}y\,\mathrm{H_2} \Rightarrow \mathrm{PtSn_y/support} + 4y\mathrm{BuH} \quad (1)$$

The reaction between the monometallic Pt catalysts and $SnBu_4$ was followed by gas chromatography, which permitted to establish the total reagent consumption, and consequently, the y value that appears in reaction (1). In order to study the specificity of the interaction between the monometallic Pt catalysts and $SnBu_4$, blank experiments were conducted, in which $SnBu_4$ was contacted with the support (γ-Al_2O_3 or SiO_2). No detectable tin amounts on the support were observed.

Table 2 presents the results of TEM, TPR and XPS analysis performed on the catalysts studied. TEM results show a narrow distribution of metallic particle sizes, with a mean particle size between 1.8 and 2.2 nm for alumina supported catalysts and between 2.4 and 2.9 nm for the silica supported ones. These values are indicating a high dispersion of the alumina supported catalysts (around 60%) and that the silica supported ones have a relatively lower dispersion (around 45%). The particle size distribution of the bimetallic systems are quite similar to the corresponding monometallic ones, presenting only a small shift (0.2–0.5 nm) compatible with a selective deposition of tin over platinum, in agreement with previously reported results involving these kind of preparation procedures [27,28]. PtSnA1.6 submitted to four reaction–regeneration cycles presented a mean particle size of only 0.1 nm higher than PtSnA1.6 fresh catalyst; this value indicates the absence of sintering phenomena. TPR diagrams show two main peaks of hydrogen consumption, in the regions of 75–110 and 360–440 °C, assigned to a weak and a strong metal support interaction, respectively [29].

XPS results show that platinum is completely reduced in all the samples studied, because the spectra contain only one peak corresponding to Pt centered around 71 eV (Pt $4f_{7/2}$)

Table 2
TEM, TPR and XPS results for PtS, PtA, PtSnA and PtSnS catalysts

Catalyst	d_{TEM} (nm)	TPR (°C)		Pt $4d_{5/2}$	Pt $4f_{7/2}$	Sn $3d_{5/2}$	$Sn(0)/Sn^{TOTAL}$	Sn(0)/Pt
		LT	HT					
PtA	1.8	75	360	314.8	–	–	–	–
PtS	2.4	100	440	–	71.6	–	–	–
PtSnA0.4	2.0	75	360	313.6	–	486.8, 483.8	0.39	0.16
PtSnA1.6	2.2	90	380	314.0	–	487.2, 484.0	0.22	0.35
PtSnA1.6 postreaction	2.3	nd	nd	314.0		487.1, 484.0	0.20	0.32
PtSnS0.4	2.8	110	440	–	70.9	487.0, 485.0	0.69	0.28
PtSnS0.7	2.9	110	440	–	70.6	487.1, 484.6	0.66	0.46

d_{TEM} (nm): mean particle size; LT and HT: low and high temperatures hydrogen consumption peaks in TPR diagrams, respectively.

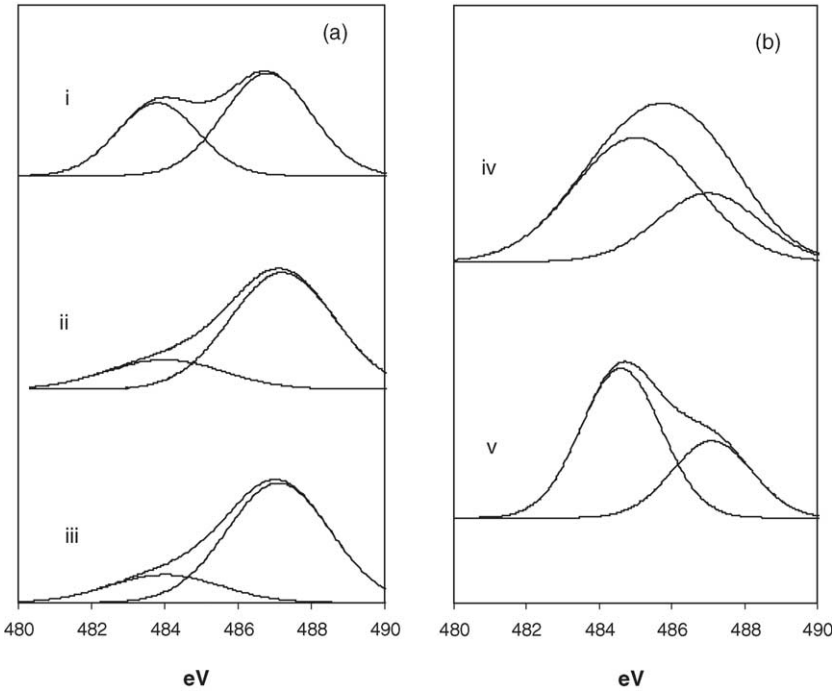

Fig. 1. XPS spectra of Sn $3d_{5/2}$ level for bimetallic catalysts: (a) PtSn/γ-Al_2O_3, (i) PtSnA0.4, (ii) PtSnA1.6 and (iii) PtSnA1.6 postreaction; (b) PtSn/SiO_2 catalysts, (iv) PtSnS0.4 and (v) PtSnS0.7.

and 314 eV (Pt $4d_{5/2}$), for silica and alumina supported catalysts, respectively. The references values were taken from the NIST X-ray photoelectron spectroscopy database [30]. In tin modified systems, a downward shift of ca. 1 eV in the binding energy of platinum was observed with respect to the corresponding monometallic catalysts. Concerning tin oxidation state, the Sn $3d_{5/2}$ peak obtained by XPS contains two contributions (Fig. 1). The first with a binding energy of around 484 eV is assigned to Sn(0) according to the well determined values obtained by Rodriguez et al. (484.9 eV) [31]; the second contribution corresponds to Sn(II,IV), with a binding energy centered around 487 eV [30]. Results obtained for the fraction of metallic tin with respect to total tin ($Sn(0)/Sn^{TOTAL}$) and Sn(0)/Pt ratio are also presented in Table 2. Fresh alumina supported bimetallic catalysts showed a $Sn(0)/Sn^{TOTAL}$ ratio between 0.2 and 0.4, whereas for silica supported catalysts this ratio is between 0.6 and 0.7. XPS analysis of PtSnA1.6 postreaction sample showed, with regard to Pt and Sn, that the nature of the bimetallic phase is not appreciably modified after four cycles of reaction–regeneration.

PtSnA0.4 and PtSnA1.6 were studied by EXAFS in order to determine the local structure around Pt atoms. PtSnA1.6 sample was also studied after four reaction–regeneration cycles to observe how the clusters were modified by the treatments and to study the stability of the catalyst. Fig. 2 shows the Pt L_3-edge k^2-weighted EXAFS functions (left) and their corresponding k^2-weighted Fourier transforms (right) of PtO_2 and Pt foil used as references. For comparison purpose, PtSnS0.7 sample was also studied. Fig. 3 shows the Pt L_3 EXAFS spectra of fresh PtSnA0.4 and PtSnA1.6 catalysts and that of PtSnS0.7. From the Fourier transforms it can be seen that no peak is present in the position corresponding to a Pt–O shell in any sample, indicating that there are no oxygen atoms in the first coordination shells of Pt in the catalysts. This confirms the complete reduction of Pt in all samples, in agreement with XPS results. Great differences are observed in the spectra corresponding to the two fresh samples supported on γ-Al_2O_3. PtSnA0.4 has a spectrum similar to that of Pt foil having one peak at 2.6 Å in the Fourier transform (without phase correction) showing that Pt is completely reduced forming metallic clusters and no other Pt phase would be present. The EXAFS spectrum PtSnA1.6 shows differences to that of Pt foil and two peaks are clearly seen in the Fourier transform at 2.0 and 2.5 Å (without phase correction) what could be indicating that two types of scatterers atoms are

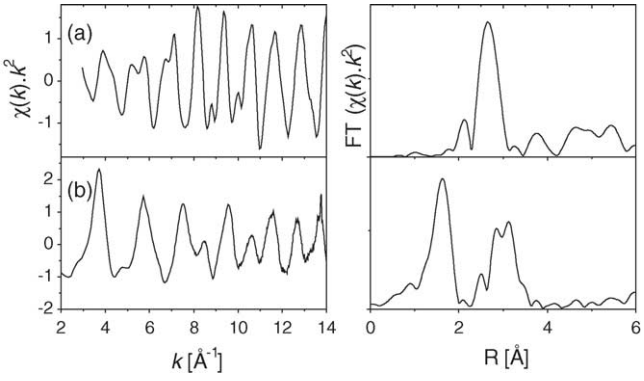

Fig. 2. Left column: Pt L_3-edge k^2-weighted EXAFS functions of (a) Pt foil and (b) PtO_2 used as references; right column: of their corresponding k^2-weighted Fourier transforms.

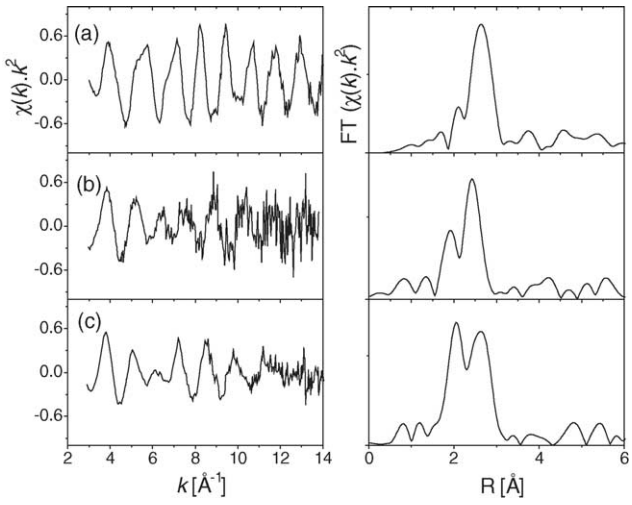

Fig. 3. Left column: Pt L_3-edge k^2-weighted EXAFS functions of (a) PtSnA0.4, (b) PtSnA1.6 and (c) PtSnS0.7 fresh catalysts; right column: their corresponding k^2-weighted Fourier transforms.

present in the first coordination shells of Pt atoms. Something similar is observed for PtSnS0.7. As it can be observed in Fig. 3, the only difference between PtSnS0.7 and PtSnA1.6 is the height of the peaks, which could be indicating differences in the average coordination numbers of the two different scatterers around Pt.

Fig. 4 shows the EXAFS spectra and their corresponding Fourier transforms of the PtSnA1.6 catalyst after one and four reaction–regeneration cycles. No large differences are observed in the Fourier transforms of these samples after the reaction–regeneration cycles and it can be seen that the spectra are similar to that of the fresh sample showing two peaks in their Fourier transforms with a slight change in the intensity of the peaks.

To quantitatively analyze these data, the main peaks of each transform were analyzed by a standard fitting procedure [32]. In this way, the distance R, the coordination number N and the Debye–Waller factor for each shell were obtained. Two shells were used in the fits of all samples, one corresponding to a Pt–Sn coordination and the other to a

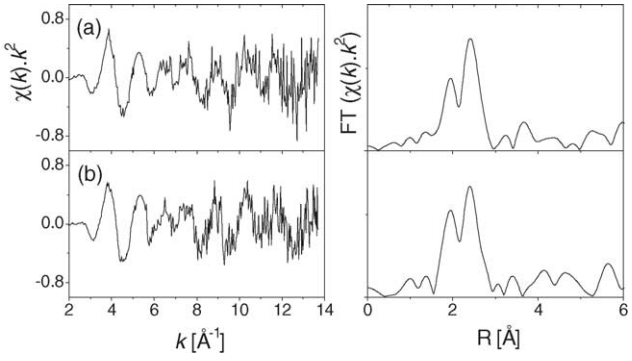

Fig. 4. Left column: Pt L_3-edge k^2-weighted EXAFS functions of PtSnA1.6 catalyst after (a) one regeneration cycle and (b) after four regeneration cycles; right column: their corresponding k^2-weighted Fourier transforms.

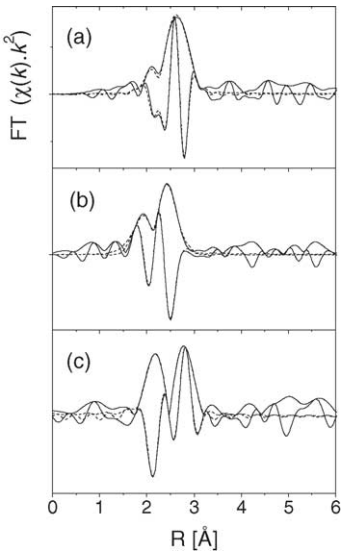

Fig. 5. Amplitude and imaginary part (solid lines) of the k^2-weighted Fourier transforms of Pt L_3-edge EXAFS spectra: (a) PtSnA0.4, (b) PtSnA1.6 and (c) PtSnS0.7 fresh catalysts and the corresponding fitted EXAFS functions (dashed lines).

Pt–Pt coordination. The phase shifts and the amplitude functions for Pt–Pt and Pt–Sn shells were calculated using the FEFF program [25] using the PtSn alloy structure [26].

Figs. 5 and 6 shows the fits performed in R-space of the experimental data. Table 3 shows the results from the EXAFS analysis performed on the Fourier transforms in the range k = 1.6–3.0 Å. It is observed that in the fresh PtSnA0.4 catalyst (with Sn/Pt = 0.4 and Sn(0)/Pt = 0.16) only one shell of Pt atoms was needed to fit the experimental data with an average coordination number of 9. For the fresh catalysts with higher tin contents (PtSnA1.6 and PtSnS0.7; Sn(0)/Pt = 0.35 and 0.46, respectively) two coordination shells are found around Pt atoms. One shell corresponds to Sn atoms and the other one to Pt atoms. The presence of the Pt–Sn coordination shell is an evidence of the existence of a PtSn alloy in the catalysts. The Pt–Pt coordination can be produced by the same PtSn alloy or by small Pt clusters not

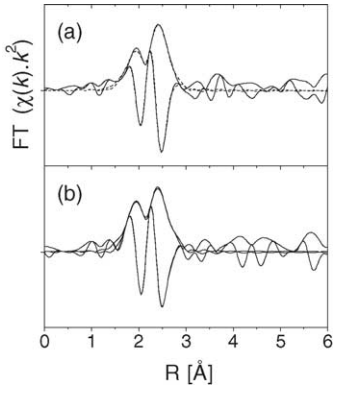

Fig. 6. Amplitude and imaginary part (solid lines) of the k^2-weighted Fourier transforms of Pt L_3-edge EXAFS spectra of PtSnA1.6 catalyst after (a) one regeneration cycle and (b) four regeneration cycles and their corresponding fitted EXAFS functions (dashed lines).

Table 3
Results of EXAFS analysis

Catalyst	Pt–Sn coordination			Pt–Pt coordination		
	N	R (Å)	σ^2 (Å^2)	N	R (Å)	σ^2 (Å^2)
PtSnA0.4 (fresh)	–	–	–	9.0 (5)	2.74 (2)	7.1×10^{-3} (5)
PtSnA1.6 (fresh)	2.7 (3)	2.59 (2)	7.2×10^{-3} (5)	1.4 (3)	2.59 (2)	7.7×10^{-3} (5)
PtSnS0.7 (fresh)	2.7 (3)	2.68 (1)	5.5×10^{-3} (5)	1.8 (2)	2.71 (1)	3.8×10^{-3} (5)
PtSnA1.6 (postreaction, first cycle)	2.4 (3)	2.59 (2)	6.6×10^{-3} (5)	1.3 (3)	2.61 (2)	6.8×10^{-3} (5)
PtSnA1.6 (postreaction, fourth cycle)	2.1 (3)	2.59 (2)	4.8×10^{-3} (5)	1.5 (3)	2.60 (2)	4.5×10^{-3} (5)

N represents the average coordination number for the coordination shell, R the interatomic distance and σ^2 the Debye–Waller factor.

alloyed to Sn. It is seen that through the regeneration processes the Pt–Sn shell is present in the catalyst showing the stability of the alloy. There is a small decrease in the coordination number on the Pt–Sn pair after the fourth regeneration cycle while the Pt–Pt coordination number increases, although the change is small and could be included in the experimental error.

As a test method, the catalysts studied in this work were submitted to the dehydrogenation reaction of isobutane to isobutene. Table 4 summarizes the results of activity and selectivity obtained after 4 h on stream, with a feed of H_2/isobutane: 3/1. It must be indicated that the selectivity to isobutene for the monometallic catalysts is very low, due to the formation of cracking and isomerization products. The addition of small quantities of tin notably modifies this selectivity by a strong inhibition of cracking reactions. As well as cracking reactions, isomerization reactions are also catalyzed by metallic active sites, nevertheless, the most important active sites for these reactions are the acid sites of the support. γ-Al_2O_3 has acid sites that are stronger than those of SiO_2, that is why the silica supported bimetallic catalysts present a higher selectivity to isobutene (>99% for PtSnS0.4). When γ-Al_2O_3 is employed as support, its modification by the addition of alkaline or alkaline-earth ions allows to obtain the same level of selectivity to isobutene as with silica, as it has been reported in previous works of our group [5,22].

From the values of reaction rate presented in Table 4, it can be concluded that monometallic catalysts are more active than the bimetallic ones. The difference observed between PtA and PtS can be assigned to the higher dispersion of the alumina supported catalyst.

The catalytic performance of the alumina supported PtSn systems can be analyzed as a function of the amount of tin added. Taking the reaction rate of PtA as reference, an initial addition of tin causes a diminution in the reaction rate. Then, as Sn/Pt ratio increases, the reaction rate increases and passes through a maximum for Sn/Pt between 0.4 and 0.8. The values for the reaction rate for silica supported bimetallic catalysts studied in this work (PtSnS0.4 and PtSnS0.7), are in the region where the reaction rate decreases with Sn/Pt ratio.

One of the most important requirements for these catalysts is their stability and regenerability. Previous studies carried out with Pt/γ-Al_2O_3 under the same conditions stated in Table 4, showed that this system lost approximately 50% of its initial activity after 4 h on stream, while bimetallic PtSn/γ-Al_2O_3 showed only a slight diminution of its activity after 8 h under reaction [3,8]. With the aim of verifying if this behavior could be observed under more severe conditions, we tested the stability and regenerability of PtSnA0.4 and PtSnA1.6 feeding the reactor with pure isobutane; for these conditions, the deactivation is accelerated. To quantify the deactivation of the catalysts, an activity coefficient (a) is defined as the ratio between the reaction rate at time t on stream and the initial reaction rate for the fresh catalyst. Fig. 7 displays the variation of the activity coefficient as a function of time on stream. As it can

Table 4
Reaction rate (R) and selectivity to cracking products ($S_{cracking}$), isobutene ($S_{isobutene}$) and isomerization products ($S_{isomerization}$) for all the studied catalysts

Catalysts	$S_{cracking}$ (%)	$S_{isobutene}$ (%)	$S_{isomerization}$ (%)	R (mmol g_{Pt}^{-1} s^{-1})
PtS	35	57	8	2.10
PtA	20	53	27	2.50
PtSnS0.4	<1	>99	~0	0.90
PtSnS0.7	<1	>99	~0	0.44
PtSnA0.05	9	66	25	1.50
PtSnA0.1	6	71	23	1.58
PtSnA0.4	3	76	21	1.90
PtSnA0.8	1	82	17	1.79
PtSnA1.6	<1	90	9	1.68

For experimental conditions, see the text.

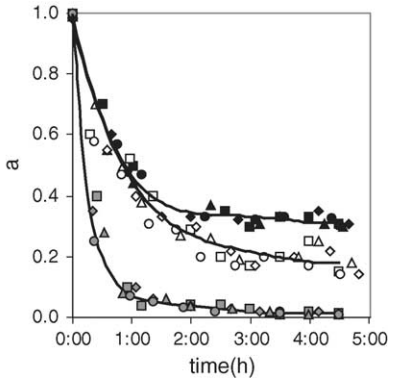

Fig. 7. Activity coefficient (a) as a function of time on stream (h): (□) cycle 1 (fresh); (◇) cycle 2; (△) cycle 3; (○) cycle 4; dark field: PtSnA1.6; white field: PtSnA0.4; grey field: PtA. For experimental conditions, see the text.

be seen, the addition of tin notably enhances the stability of the catalysts. Also, this figure shows that the catalysts can be regenerated, recovering the activity level of the fresh sample. This means that the nature of the active phase is recovered after each reaction–regeneration cycle, in agreement with the XPS and EXAFS results found for fresh and postreaction PtSnA1.6 sample.

4. Discussion

Results obtained by TPR, XPS and EXAFS clearly established the complete reduction of platinum in mono and bimetallic catalysts, both for silica and alumina supports. Blank experiments demonstrated that, under the reaction conditions employed in the preparation of tin modified catalysts using SOMC/M techniques, tin was not detectable on the support. After the activation step at 500 °C in a H_2 flow, butyl groups are completely eliminated and the bimetallic catalyst is obtained [28,33]. In this case, XPS demonstrated the existence of ionic tin, whose origin may be assigned to the migration of part of the tin, initially deposited onto the platinum via the reaction with $SnBu_4$, to the platinum–support interface where it could be forming aluminate or silicate, as it has been observed for RhSn, for instance [27]. The XPS $Sn(0)/Sn^{TOTAL}$ ratio is lower for alumina supported than for silica supported catalysts (Table 2). In silica supported catalysts, the percentage of Sn(0) is about 60–70%, despite the concentration of tin in the sample, whereas for alumina supported catalysts this percentage is under 40%. In this latter systems, the contribution of Sn(0) diminishes with increasing global Sn/Pt ratio, causing that even for PtSnA1.6, Sn(0)/Pt ratio does not exceed a value of 0.35. This behavior can be surely related to the higher surface activity of alumina compared to silica, which would result in a more favorable condition to the formation of the above mentioned tin aluminate compounds. The higher dispersion of PtA catalyst, also favors the formation of these compounds, due to the higher platinum–support interface.

Concerning the downwards shift of approximately 1 eV observed in the BE of Pt in all the bimetallic catalysts studied, it would be indicative of the existence of an electronic effect of tin over platinum, in agreement with previously published results for $PtSn/SiO_2$ catalysts prepared by Stagg et al. [2]. Studies carried out by Shen et al. from quantum chemical calculations employing density functional theories (DFT) for Pt_{19} and $Pt_{16}Sn_3$ clusters indicate that tin donates electrons to the 6sp and 5d orbitals of platinum [34]. Rodríguez et al. investigated platinum–tin surface alloys using synchrotron-based high resolution photoemission and ab initio self consistent field calculations and concluded that Pt–Sn bond involves a Sn(5s,5p) → Pt(6s,6p) charge transfer together with a Pt(5d) → Pt(6s,6p) rehybridization [31,35]. In this same sense, in a previous study of a $PtSn/SiO_2$ system by Pt-$L_{2,3}$ XANES, the existence of an electronic effect was also explained by means of the d → s, p rehybridization process taking place in PtSn three-dimensional small nanoclusters leading to an increase in the number of Pt 5d holes [36].

The EXAFS profiles of PtSnA0.4 and PtSnA1.6 samples exhibit some differences (Fig. 3). The catalyst with the lowest tin content (PtSnA0.4) has a spectrum similar to that of Pt foil, presenting a decrease of the average coordination number with respect to the Pt bulk that indicates the small size of the metallic clusters. When small particles are analyzed by EXAFS, the average coordination number fitted from the spectra is smaller than that of the bulk, because of the high proportion of atoms in the surface. A simple model can be used to estimate the size of these clusters supposing spherical shape. Fig. 8 shows the average coordination number of ideal spherical Pt clusters as a function of the radius of the cluster. It is seen that the average coordination number increases rapidly for small particles and approaches asymptotically the value of the bulk, which is 12. From this curve, the size of the clusters in our sample can be estimated using the fitted coordination number. The obtained radius of the clusters is between 8 and 10 Å. For the fresh catalysts PtSnA1.6 and PtSnS0.7 two coordination shells are found around Pt atoms. One shell corresponds to Sn atoms and the other one to Pt atoms, being the presence of the Pt–Sn coordination shell an evidence of the existence of a PtSn alloy in the catalysts. The Pt–Pt coordination can be produced by the same PtSn alloy or by small Pt clusters not alloyed to Sn. The information obtained from the EXAFS fits permits to know the structural characteristics of the bimetallic clusters that Pt and Sn atoms are forming in the catalyst. As it has been reported that PtSn and Pt_3Sn are the most abundant alloys in Pt–Sn bimetallic systems [37] we will consider these two alloys in our analysis. In Pt_3Sn, Pt atoms have 12 first-neighbors Pt and 4 first-neighbors Sn at a distance of 2.828 Å [38]. If the structure present in our catalyst were this type of alloy one would expect a relation of Pt and Sn atoms in the first coordination of 3 to 1. This is clearly not the case from our fits. Moreover, the distances are not equal for the two types of atoms as in the alloy. Thus, we would not expect our bimetallic particles over γ-Al_2O_3 and over SiO_2 to have the structure of this alloy. In contrast, in

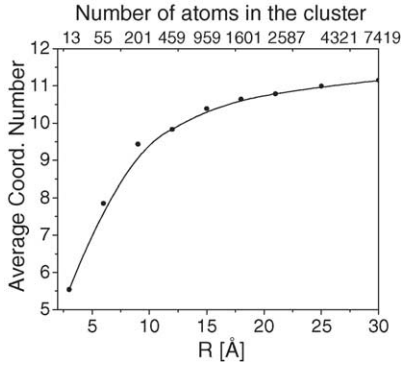

Fig. 8. Average coordination number of Pt atoms for spherical Pt clusters.

PtSn alloy, Pt has two Pt atoms at 2.72 Å and six Sn atoms at 2.73 Å. In this case one would expect a coordination number relation for Pt and Sn of 1:3. This is closer to the relation found in our case. However, the distances for each coordination shell are inverted. That is, Sn atoms are closer than Pt atoms in our samples, contrary to what happens in the alloy, though differences are small. This can be understood in terms of the coexistence of two different phases in the catalyst: a PtSn alloy and some unalloyed Pt particles. The unalloyed Pt phase would contribute to the Pt–Pt shell increasing both its coordination number and its distance (the distance of Pt–Pt pairs in the bulk is 2.77 Å). This would also explain why the relation between coordination numbers for the shells Pt–Pt and Pt–Sn is not 1:3 as expected for the PtSn alloy. In addition, Borgna et al. [39] have shown that the presence of the peak at 2.15 Å found in our radial distribution function is not only a fingerprint for Pt–Sn interactions, but also the evidence of the existence of unalloyed Pt. The decrease of the average coordination number from that of the bulk can be explained because of the small size of the clusters having an important contribution from atoms on the surface.

The coexistence of an unalloyed metallic Pt phase can be confirmed considering the quantity of Pt and Sn atoms in the PtSnA1.6 and PtSnS0.7 catalysts. Taking into account XPS results that show that the Sn(0)/Pt $\sim$ 0.3–0.5, there are between twice and three times more Pt atoms than Sn atoms available to form the alloy. In this analysis we have considered the simplest configuration which is consistent with our results. Of course, one cannot rule out the coexistence of different alloys with different Pt/Sn ratios. However, even if that was the case, the most important conclusion from this analysis is the coexistence of a Pt–Sn alloy with some segregated metallic Pt. As the stoichiometry of the alloy is PtSn (ratio Sn/Pt = 1), the rest of Pt atoms should be segregated forming small metallic clusters as no other type of scatterer is found in our EXAFS results indicating that there is no other Pt phases present.

EXAFS fits do not show evidence of changes in the structure around Pt atoms after the different regeneration cycles. From the results shown in Table 3 it can be seen that the Pt and Sn shells are present after one and four reaction–regeneration cycles and the quantity and distance of both scatterers around Pt atoms are kept almost unchanged. A small variation in the coordination numbers is observed after four regeneration cycles but this difference could be included in the experimental error. These results are a clear evidence of the stability of the alloy and the metallic Pt phase in the catalysts.

The absence of Pt–Sn alloy in the PtSnA0.4 catalyst can be also explained in terms of the quantity of Sn available to form the alloy. XPS results show that approximately 60% of Sn atoms are ionic, having only ca. 40% of Sn atoms available to form the alloy, which leads to a Sn(0)/Pt ratio of approximately 0.15. That is, there are approximately seven times Pt atoms than Sn atoms to form the alloy. In this way, if some alloy were present it would contribute with less than 15% of the total EXAFS signal and could not be resolved.

A study of dehydrogenation of isobutane for all the catalysts was preformed, under the conditions indicated in the experimental section. Tin modified Pt catalysts showed an important inhibition of cracking reactions, which is a structure sensitive reaction, a result that can be assigned to the ''destruction'' of platinum ensembles caused by the presence of metallic tin [2–4,7–10]. The inhibiting effect of tin is observed even for the catalysts with low Sn/Pt ratio, as it arises from the data presented in Table 4. For instance, for PtSnA1.6 (Sn(0)/Pt = 0.35) and PtSnS0.4 (Sn(0)/Pt = 0.28), the selectivity to cracking products is under 1%. EXAFS results revealed that, when the Sn(0)/Pt ratio increases, it appears a PtSn alloy, which would be responsible for the destruction of the platinum active sites leading to cracking reactions. In this sense, the alloy behaves in a way similar to that of isolated Sn(0).

The direct dehydrogenation of light paraffins is carried out under severe operating conditions favorable to the deactivation of the catalysts by sintering and/or coke formation (high temperatures, low H/C ratio). TEM data of the studied catalysts led to the conclusion that, under the experimental conditions employed here, sintering deactivation mechanism is not important, because the mean particle size of the fresh and postreaction samples are about the same. As an example, see the data for PtSnA1.6 in Table 2. Thus, coke formation is surely the main deactivation process that takes place during the dehydrogenation reaction. In Fig. 7, it is depicted how the activity coefficient diminishes as a function of time for PtA, PtSnA0.4 and PtSnA1.6 catalysts, being the deactivation lower for the sample with the highest Sn/Pt ratio. This is in agreement with the fact that tin provokes a notably diminution in the quantity of coke deposited during the dehydrogenation reaction, as has been previously demonstrated [8]. The coke formation process is favored by reactions that, the same as the cracking reactions, are structure sensitive; that is why the decrease of the size of platinum ensembles, either by isolated Sn(0) or by PtSn alloy, enhances the stability of the catalytic system. The electronic modifications introduced by the presence of tin, also promote the stability of the bimetallic systems, by inhibiting coke formation reactions. In fact, the increase of the electronic density on the Pt atoms (observed by XPS) causes the decrease of the interaction between coke precursors and the active site, due to the repulsion electronic effects leading to the diminution of adsorption energy of these coke precursors. The addition of tin to Pt/SiO_2 decreases the initial heat of isobutene adsorption from 185 kJ mol^{-1} on Pt/SiO_2 to 125 kJ mol^{-1} on $PtSn/SiO_2$. Accordingly, the addition of tin to Pt/SiO_2 appears to suppress the decomposition of adsorbed olefins to more highly dehydrogenated species. It has also been suggested that tin favors the transport of coke from active sites to the support on PtSn/γ-Al_2O_3 catalysts [10].

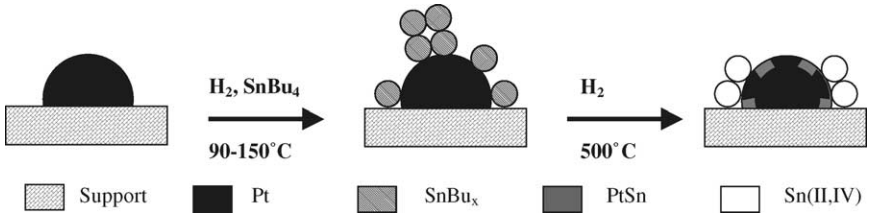

Scheme 1. Representation of catalytic surface for PtSn catalysts.

An aspect to be highlighted related to PtSn/γ-Al_2O_3 catalysts, is their stability facing successive reaction–regeneration cycles. The experimental points in Fig. 7 shows a marked reproducibility in the activity coefficient values corresponding to different reaction–regeneration cycles, in agreement with the similarities found in the nature of the fresh and postreaction phases, as measured by XPS and EXAFS.

These results can surely be ascribed to the preparation procedure employed, derived from SOMC/M. One plausible explanation for the results presented in this paper could be that as this preparation method generates such strong interaction between Pt and Sn, well-defined bimetallic phases are obtained, that are stable facing several reaction–regeneration cycles. Previously published results involving PtSn/γ-Al_2O_3 catalysts prepared using conventional methods showed that several deactivation–regeneration cycles decreased the activity of the catalysts [1,40].

The evolution of the bimetallic phases through the different steps of preparation and activation, could be represented by Scheme 1. As it was already presented, the first step consisted of the reaction between $SnBu_4$ and the monometallic platinum catalyst in a H_2 atmosphere and temperatures between 90 and 150 °C. Upon reduction at 500 °C, the organic fragments are eliminated. Considering the Sn/Pt atomic ratios employed in the present study, at the end of the activation step, the active phase is determined by the fraction of free metallic platinum forming clusters of small dimensions, isolated by PtSn alloys.

In Fig. 9 the reaction rate values are depicted as a function of the Sn(0)/Pt ratio. For all the studied catalysts there is a diminution in the reaction rate as the Sn(0)/Pt increases.

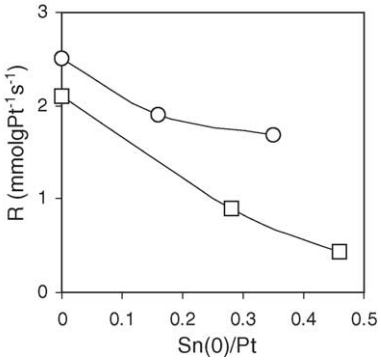

Fig. 9. Reaction rate as a function of Sn(0)/Pt: (□) PtSn/SiO_2; (○) PtSn/γ-Al_2O_3.

Among the catalysts analyzed in this work, the one with the highest Sn(0)/Pt ratio (PtSnS0.7, Sn(0)/Pt = 0.46) is the system with the lowest reaction rate. For alumina supported PtSn catalysts, the Sn(0)/Pt ratio varies with the amount of tin added in a less pronounced way than for silica supported catalysts (see Table 2) and, accordingly, the dehydrogenation rate is less sensitive to the Sn/Pt ratio. Considering the fundamental catalytic properties (activity, selectivity, stability) as a whole, PtSnA1.6 catalyst (Sn/Pt = 1.6; Sn(0)/Pt = 0.35) resulted the best system among those studied here.

Taking into account the image of the surface represented in Scheme 1, where small Pt clusters coexist with PtSn alloy, and the catalytic results obtained, it seems reasonable to accept that the PtSn alloy is not active in the dehydrogenation reaction, or at least its activity level is notably lower than that of Pt clusters. It is likely that PtSn alloy has the mission of inhibiting cracking and coke formation reactions and of ‘‘cleaning’’ the active phase, by favoring the migration of highly dehydrogenated species to the support. This last process might be helped by the presence of ionic tin at the platinum–support interface. The proportion of the PtSn alloy must be kept relatively low with respect to non-alloyed platinum, so that the dehydrogenation activity would not be affected. Yining et al. studied the dehydrogenation of *n*-butane with PtSn/γ-Al_2O_3 catalysts, prepared by impregnation with an aqueous solution of (H_2PtCl_6 + $SnCl_2$) and having a Sn/Pt ratio of 3 [1]. In agreement with the above mentioned results, they observed that the dehydrogenation activity of the catalyst was diminished with the increase in the amount of the PtSn alloy in the course of several coking–regeneration cycles. Our catalytic, XPS and EXAFS results show that bimetallic PtSn/γ-Al_2O_3 catalysts, prepared via SOMC/M techniques, can be submitted to several sequential reaction–regeneration cycles, recovering the same level of initial activity each time. This fact could be assigned to the close interaction between tin and platinum, leading to a well defined active phase as it is shown in Scheme 1, avoiding in this way the ‘‘waste’’ of the metal promoter that could play a negative role after several reaction–regeneration cycles.

5. Conclusions

Well defined supported PtSn catalysts were prepared by surface organometallic reactions and were characterized by TEM, XPS and EXAFS techniques and catalytic dehy-

drogenation of isobutane. The main conclusions can be summarized as follows:

- XPS results show that in supported PtSn catalysts, tin is found under the form of Sn(0) and Sn(II,IV). The contribution of Sn(0) with respect to Sn^{TOTAL} is lower for alumina supported than for silica supported catalysts. In all tin modified platinum catalysts, our results show a downwards shift of approximately 1 eV in the BE of Pt. This fact would be indicative of the existence of an electronic effect, suggesting that there is an electron charge transfer from tin to platinum.
- EXAFS experiments in PtSn supported samples allow to demonstrate the existence of a PtSn alloy diluting metallic Pt atoms for the higher Sn(0)/Pt ratios, in our case approximately 0.3. This PtSn alloy seems to be not active in the dehydrogenation reaction, and would have the mission of inhibiting cracking and coke formation reactions and of ''cleaning'' the active phase. The proportion of the PtSn alloy must be kept relatively low with respect to non-alloyed platinum, so that the dehydrogenation activity would not be affected.
- Catalytic, XPS and EXAFS results performed in this work, show that bimetallic PtSn/γ-Al_2O_3 catalysts, prepared via SOMC/M techniques, can be submitted to several sequential reaction–regeneration cycles, recovering the same level of initial activity each time and that the nature of the catalytic surface remains practically without modifications. This fact could be assigned to the close interaction between tin and platinum, leading to a well defined active phase, avoiding in this way the ''waste'' of the metal promoter that could play a negative role after several reaction–regeneration cycles.

Acknowledgments

This work has been sponsored by the Consejo Nacional de Investigaciones Científicas y Técnicas (CONICET, Argentina), the Agencia Nacional de Promoción Científica y Técnica (PICT #14-04378, Argentina), the Fundación Antorchas (Project #14116-120, Argentina) and the LNLS (Project D04B-XAS #2370/03, Campinas, SP, Brazil). The authors thank Guillermo Bertolini for performing the isobutane dehydrogenation tests.

References

[1] F. Yining, X. Zhusheng, Z. Jingling, L. Liwu, Stud. Surf. Sci. Catal. 69 (1991) 683.
[2] S.M. Stagg, C.A. Querini, W.E. Alvarez, D.E. Resasco, J. Catal. 168 (1997) 75.
[3] M.L. Casella, G.J. Siri, G.F. Santori, O.A. Ferretti, M. Ramírez de Agudelo, Langmuir 13 (2000) 5639.
[4] G.F. Santori, M.L. Casella, G.J. Siri, O.A. Ferretti, J.L.G. Fierro, Stud. Surf. Sci. Catal. 130 (2000) 3897.
[5] G.J. Siri, M.L. Lladó, M.L. Casella, O.A. Ferretti, in: Proceedings of the XVIII Simposio Iberoamericano de Catálisis, vol. 1, Venezuela, 2002, p. 2523.
[6] F.M. Brinkmeyer, D.F. Rohr, US Patent 4,866,211 (1987).
[7] E. Merlen, P. Beccat, J.C. Bertolini, P. Delichère, N. Zanier, B. Didillon, J. Catal. 159 (1996) 178.
[8] G.J. Siri, M.L. Casella, G.F. Santori, O.A. Ferretti, Ind. Eng. Chem. Res. 36 (1997) 4821.
[9] J.M. Hill, R.D. Cortright, J.A. Dumesic, Appl. Catal. A: Gen. 168 (1998) 9.
[10] R.D. Cortright, J.M. Hill, J.A. Dumesic, Catal. Today 55 (2000) 213.
[11] Z. Paál, A. Gyory, I. Uszkurat, S. Olivier, M. Guérin, C. Kappenstein, J. Catal. 168 (1997) 2463.
[12] C. Kappenstein, M. Guérin, K. Lázár, K. Matusek, Z. Paál, J. Chem. Soc., Faraday Trans. 94 (1998) 2463.
[13] C. Vértes, E. Tálas, I. Czakó-Nagy, J. Ryczkowski, S. Göbölös, A. Vértes, J. Margitfalvi, Appl. Catal. 68 (1991) 149.
[14] J. Llorca, N. Homs, J. León, J. Sales, J.L.G. Fierro, P. Ramírez de la Piscina, Appl. Catal. A: Gen. 189 (1999) 77.
[15] M.C. Román-Martínez, D. Cazorla-Amorós, H. Yamashita, S. de Miguel, O.A. Scelza, Langmuir 16 (2000) 1123.
[16] C. Audo, J.F. Lambert, M. Che, B. Didillon, Catal. Today 65 (2001) 157.
[17] L. Bednarova, C.E. Lyman, E. Rytter, A. Holmen, J. Catal. 211 (2002) 335.
[18] F.M. Dautzemberg, J.N. Helle, P. Biloen, W.M.H. Sachtler, J. Catal. 69 (1980) 119.
[19] K. Balakrishnan, J. Schwank, J. Catal. 127 (1991) 287.
[20] H. Lieske, J. Völter, J. Catal. 90 (1984) 96.
[21] Y. Li, K.J. Klabunde, B.H. Davis, J. Catal. 128 (1991) 1.
[22] G.J. Siri, M.L. Casella, O.A. Ferretti, J.L.G. Fierro, Stud. Surf. Sci. Catal. 139 (2001) 287.
[23] T. Ressler, S.L. Brock, J. Wong, S.L. Suib, J. Phys. Chem. B 103 (1999) 6407.
[24] T. Ressler, J. Synch. Rad. 5 (1998) 118.
[25] S.I. Zabinsky, J.J. Rehr, A. Ankudinov, R.C. Albers, M.J. Eller, Phys. Rev. B 52 (1995) 2995.
[26] I.R. Harris, M. Norman, A.W. Bryant, J. Less-Common Met. 16 (1968) 427.
[27] O.A. Ferretti, C. Lucas, J.P. Candy, J.M. Basset, B. Didillon, F. Le Peltier, J. Mol. Catal. 103 (1995) 125.
[28] G.F. Santori, M.L. Casella, G.J. Siri, H.R. Adúriz, O.A. Ferretti, Appl. Catal. A: Gen. 197 (2000) 141.
[29] C. Kappenstein, M. Saouabé, M. Guérin, P. Marecot, I. Uszkurat, Z. Paál, Catal. Lett. 31 (1995) 9.
[30] C.D. Wagner, NIST X-ray Photoelectron Spectroscopy Database, Gathersburg, 1989.
[31] J.A. Rodriguez, T. Jirsak, S. Chaturvedi, J. Hrbek, J. Am. Chem. Soc. 120 (1998) 11149.
[32] D.C. Koningsberger, R. Prins (Eds.), X-ray Absorption Techniques of EXAFS, SEXAFS and XANES, Wiley, New York, 1988.
[33] G.F. Santori, M.L. Casella, O.A. Ferretti, J. Mol. Catal. A 186 (2002) 223.
[34] J. Shen, J.M. Hill, R.M. Watwe, B.E. Spiewak, J.A. Dumesic, J. Phys. Chem. B 103 (1999) 3923.
[35] J.A. Rodriguez, S. Chaturvedi, T. Jirsak, J. Hrbek, J. Chem. Phys. 109 (1998) 4052.
[36] J.M. Ramallo López, G.F. Santori, L. Giovanetti, M.L. Casella, O.A. Ferretti, F.G. Requejo, J. Phys. Chem. B 107 (2003) 11441.
[37] G. Meitzner, G.H. Via, F.W. Lytle, S.C. Fung, J.H. Sinfelt, J. Phys. Chem. 92 (1988) 2925.
[38] M. Ellner, J. Less-Common Met. 78 (1981) 21.
[39] A. Borgna, S.M. Stagg, D.E. Resasco, J. Phys. Chem. 102 (1998) 5077.
[40] K. Pierpauli, C.A. Querini, in: Proceedings of the XVII Simposio Iberoamericano de Catálisis, FEUP Ediçoes 1, Porto, Portugal, 2000, p. 833.